

Function Projective Synchronization of Discrete-Time Chaotic Systems

Xin Li^{a,c}, Yong Chen^{a,b,c}, and Zhibin Li^{b,c}

^a Nonlinear Science Center and Department of Mathematics, Ningbo University, Ningbo 315211, China

^b Institute of Theoretical Computing, East China Normal University, Shanghai 200062, China

^c Key Laboratory of Mathematics Mechanization, Chinese Academy of Sciences, Beijing 100080, China

Reprint requests to Y. C.; E-mail: chen Yong@nbu.edu.cn

Z. Naturforsch. **63a**, 7 – 14 (2008); received July 26, 2007

First, a function projective synchronization is defined in discrete-time dynamical systems, in which the drive and response state vectors evolve in a proportional scaling function matrix. Second, based on backstepping design with three controllers, a systematic, concrete and automatic scheme is developed to investigate the function projective synchronization of discrete-time chaotic systems. With the aid of symbolic-numeric computation, we use the proposed scheme to illustrate the function projective synchronization between the 2D Lorenz discrete-time system and the Fold discrete-time system, as well as between the 3D hyperchaotic Rössler discrete-time system and the Hénon-like map. Numeric simulations are used to verify the effectiveness of our scheme. By choosing different scaling functions, the interesting attractor figures of the drive and response systems are showed in a proportional scaling function.

Key words: Function Projective Synchronization; Backstepping Design; Discrete-Time Chaotic System.

1. Introduction

Chaos (hyperchaos) synchronization has received considerable attention because of its potential applications in secure communication and complex networks, since the pioneering works of Fujisaka and Yamada [1], Pecora and Carroll [2], Pyragas [3], and Ott et al. [4]. Up to now, there exist many types of chaos synchronization in dynamical systems such as complete synchronization, partial synchronization, phase synchronization, lag synchronization, anticipated synchronization, generalized lag, anticipated and completed synchronization, antiphase synchronization [5–11]. In particular, amongst all kinds of chaos synchronization, projective synchronization in partially linear systems reported by Mainieri and Rehacek [12] is one of the most noticeable ones that evolves the drive and response vectors in a proportional scale – the vectors become proportional. Recently, some researchers [13–15] extended the projective synchronization to partially nonlinear systems, and based on their work, we have proposed the function projective synchronization (FPS) in continuous-time systems which evolve the drive and response vectors

in a proportional scaling function matrix [16]. Many powerful methods have been reported to investigate some types of chaos (hyperchaos) synchronization in continuous-time systems. In fact, many mathematical models of neural networks, biological processes, physical processes and chemical processes were defined using discrete-time dynamical systems [17–20]. Recently, more and more attention was paid to the chaos (hyperchaos) control and synchronization in discrete-time dynamical systems [21].

Backstepping design [21–24] has become a systematic and powerful method for the construction of both feedback controllers and associated Lyapunov functions. The design method has been applied to investigate control and synchronization of many continuous-time dynamical systems [24–27]. Up to now, some articles have been reported extending the backstepping design to deduce some proper controllers to investigate chaos control and synchronization in some discrete-time dynamical systems [21, 28–31]. Recently, we give a more general definition of the function projective synchronization to synchronize two different systems up to a scaling function matrix f with different initial values [16]. The corresponding framework of

synchronization is set up and used to achieve a function projective synchronization design of two different chaotic systems: the unified chaotic system and the Rössler system.

In this paper, on the lines of the function synchronization thought, we define a type of function projective synchronization in discrete-time dynamical systems. Based on the backstepping design method, we present a systematic and automatic algorithm to investigate simultaneously the FPS, via controllers between the discrete-time drive system and response system, whether it is with strict-feedback form or not. With the aid of symbolic-numeric computation, the proposed scheme is used to illustrate the FPS between the 2D discrete-time Lorenz system and the Fold discrete-time system, as well as the 3D hyperchaotic discrete-time Rössler system and the Hénon-like map. Moreover numerical simulations are used to verify the effectiveness of the proposed scheme.

This paper is arranged as follows: In Section 2, we introduce the FPS in discrete-time systems. In Section 3, we investigate the function projective synchronization in the 2D Lorenz discrete-time dynamical system and the Fold system. In Section 4, we investigate the FPS between the 3D Rössler discrete-time system and the Hénon-like map. Finally, some conclusions and discussion are given in Section 5.

2. FPS of Discrete-Time Chaotic Systems

In the following, similar to the definition of function projective synchronization in continuous-time dynamical systems, we define a FPS in discrete-time dynamical systems, and then give a Lyapunov stability theory for discrete-time dynamical systems.

Definition: For two discrete-time (chaotic or hyperchaotic) dynamical systems (i) $x(k+1) = F(x(k))$ and (ii) $y(k+1) = G(y(k)) + u(x(k), y(k))$, where $(x(k), y(k)) \in \mathbb{R}^{m+m}$, $k \in \mathbb{Z}/\mathbb{Z}^-$, and $u(x(k), y(k)) \in \mathbb{R}^m$, let (iii) $E(k) = (E_1(k), E_2(k), \dots, E_m(k)) = (x_1(k) - f_1(x(k))y_1(k), x_2(k) - f_2(x(k))y_2(k), \dots, x_m(k) - f_m(x(k))y_m(k))$ be boundary vector functions, if there exist proper controllers $u(x(k), y(k)) = (u_1(x(k), y(k)), u_2(x(k), y(k)), \dots, u_m(x(k), y(k)))^T$ such that $\lim_{k \rightarrow \infty} (E(k)) = 0$. We say that there exists function projective synchronization (FPS) between the systems (i) and (ii).

Based on the Lyapunov stability theory, for the error discrete-time (iii) generated by drive system (i) and the response system (ii), let

$L(E_1(k), E_2(k), \dots, E_m(k))|_{E_i(k) \equiv 0 (i=1,2,\dots,m)} = 0$, if $\Delta L(k) = L(k+1) - L(k) \leq 0$, with the equality holding if and only if $E_i(k) \equiv 0 (i = 1, 2, \dots, m)$. It is said that systems (i) and (ii) are function projective synchronized.

In this paper based on the backstepping design method, we would like to present a systematic, generalized and constructive scheme to seek the controllers such that the 2D Lorenz discrete-time system and the 2D Fold discrete-time system with strict-feed form, as well as the 3D hyperchaotic Rössler discrete-time system and the 3D Hénon-like map with strict-feed form are function projective synchronized.

Remark: It is necessary to point out that the controller u depends on the synchronization method chosen. When $E_i(k) = 0 (i = 1, \dots, m)$, $u = f^{-1}F - G$, where $f = \text{diag}(f_1(x(k)), \dots, f_m(x(k)))$, $u = f^{-1}F - G$ is the situation when all the error functions equal to zero and the corresponding controller is trivial. For $E_i(k) = 0$, we need only to solve the equations $(E_1(k), E_2(k), \dots, E_m(k)) = (x_1(k) - f_1(x(k))y_1(k), x_2(k) - f_2(x(k))y_2(k), \dots, x_m(k) - f_m(x(k))y_m(k)) = (0, 0, \dots, 0)$ to get the trivial controller u . So here we just consider the general condition $\lim_{k \rightarrow \infty} (E(k)) = 0$.

3. FPS of the 2D Lorenz Discrete-Time System and the Fold Discrete-Time System

Consider the Lorenz discrete-time system

$$\begin{aligned} x_1(k+1) &= (1 + \alpha\beta)x_1(k) - \beta x_1(k)x_2(k), \\ x_2(k+1) &= (1 - \beta)x_2(k) + \beta x_1^2(k), \end{aligned} \quad (3.1)$$

and the Fold system with controllers $u(x, y)$

$$\begin{aligned} y_1(k+1) &= y_2(k) + ay_1(k) + u_1(x, y), \\ y_2(k+1) &= b + y_1^2(k) + u_2(x, y), \end{aligned} \quad (3.2)$$

as the drive system and response system, respectively.

Firstly we give out the figures (Fig. 1a and Fig. 1b) of the two systems with initial variables $[x_1(0) = 0.1, x_2(0) = 0.2]$ and $[y_1(0) = -0.5, y_2(0) = -0.3]$, respectively. Here $\alpha = 1.25$, $\beta = 0.75$, $a = -0.1$, and $b = -1.7$.

In the following, we would like to realize the FPS of the Lorenz discrete-time system and the Fold discrete-time system by the backstepping design method. We choose $(f_1(x), f_2(x)) = (1, 1 + \tanh(x_2(k)))$ and $(f_1(x), f_2(x)) = (2, 2)$, respectively.

(I): Let the error states be $E_1(k) = x_1(k) - y_1(k)$, $E_2(k) = x_2(k) - (1 + \tanh(x_2(k)))y_2(k)$, here $f_1(x) =$

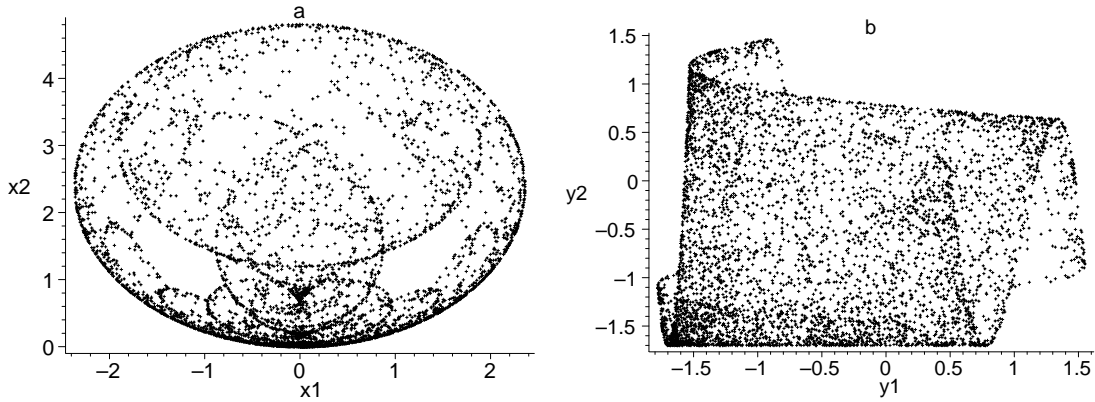


Fig. 1. (a) Lorenz discrete-time attractor; (b) Fold discrete-time attractor.

1, $f_2(x) = 1 + \tanh(x_2(k))$. Then from (3.1) and (3.2), we have the discrete-time error dynamical system

$$\begin{aligned} E_1(k+1) &= (1 + \alpha\beta)x_1(k) - \beta x_1(k)x_2(k) \\ &\quad - y_2(k) - ay_1(k) - u_1(x, y), \\ E_2(k+1) &= \beta x_1(k)^2 + (1 - \beta)x_2(k) - y_1(k)^2 - b \\ &\quad - u_2(x, y) - \tanh((1 - \beta)x_2(k) \\ &\quad + \beta x_1(k)^2)(b + y_1(k)^2 + u_2(x, y)). \end{aligned} \quad (3.3)$$

In the following based on the backstepping design and the improved ideas of [28, 30], we give a systematic and constructive algorithm to derive the controllers $u(x, y)$ step by step such that systems (3.1) and (3.2) are synchronized together.

Step 1. Let the first partial Lyapunov function be $L_1(k) = |E_1(k)|$ and the second error variable be

$$E_2(k) = E_1(k+1) - c_{11}E_1(k), \quad (3.4)$$

where $c_{11} \in \mathbb{R}$. Then we have the derivative of $L_1(k)$:

$$\begin{aligned} \Delta L_1(k) &= |E_1(k+1)| - |E_1(k)| \\ &\leq (|c_{11}| - 1)|E_1(k)| + |E_2(k)|. \end{aligned} \quad (3.5)$$

Step 2. Let

$$E_2(k+1) - c_{21}E_1(k) - c_{22}E_2(k) = 0. \quad (3.6)$$

Then with the aid of symbolic computation, from the above equations (3.4) and (3.6) we obtained the con-

trollers

$$\begin{aligned} u_1(x, y) &= (1 + \alpha\beta - c_{11})x_1(k) - \beta x_1(k)x_2(k) \\ &\quad - (a - c_{11})y_1(k) - x_2(k) \\ &\quad + y_2(k) \tanh(x_2(k)), \\ u_2(x, y) &= [(1 - \beta - c_{22})x_2(k) + \beta x_1(k)^2 - b - y_1(k)^2 \\ &\quad + (b + y_1(k)^2) \tanh((\beta - 1)x_2(k) \\ &\quad - \beta x_1(k)^2) - c_{21}x_1(k) + c_{21}y_1(k) \\ &\quad + c_{22}y_2(k)(1 + \tanh(x_2(k)))] \\ &\quad / (\tanh((\beta - 1)x_2(k) - \beta x_1(k)^2) - 1). \end{aligned} \quad (3.7)$$

Let the second partial Lyapunov function be $L_2(k) = L_1(k) + d_1|E_2(k)|$, where $d_1 > 1$, then the derivative of $L(k)$ is

$$\begin{aligned} \Delta L(k) &= L_2(k+1) - L_2(k) \\ &= \Delta L_1(k) + d_1(|E_2(k+1)| - |E_2(k)|) \\ &\leq (|c_{11}| - 1 + d_1|c_{21}|)|E_1(k)| \\ &\quad + (1 - d_1 + d_1|c_{22}|)|E_2(k)|. \end{aligned} \quad (3.8)$$

It follows that the right-hand side of (3.8) is negative definite, if the following conditions hold:

$$|c_{11}| + d_1|c_{21}| < 1, \quad d_1 - d_1|c_{22}| > 1. \quad (3.9)$$

Obviously, there exist many sets of solutions $[c_{11}, c_{21}, c_{22}]$ that satisfy (3.9). In the following we use numerical simulations to verify the effectiveness of the above-mentioned controllers. The parameters are chosen as $d_1 = 2$, $c_{11} = -0.2$, $c_{21} = -0.25$, $c_{22} = 0.4$, and the initial values of system (3.1) and (3.2) with $u = 0$ are taken as those in Figure 1. The graphs of FPS error states and the global picture of the drive and response systems are displayed in Figs. 2a, 2b and 3.

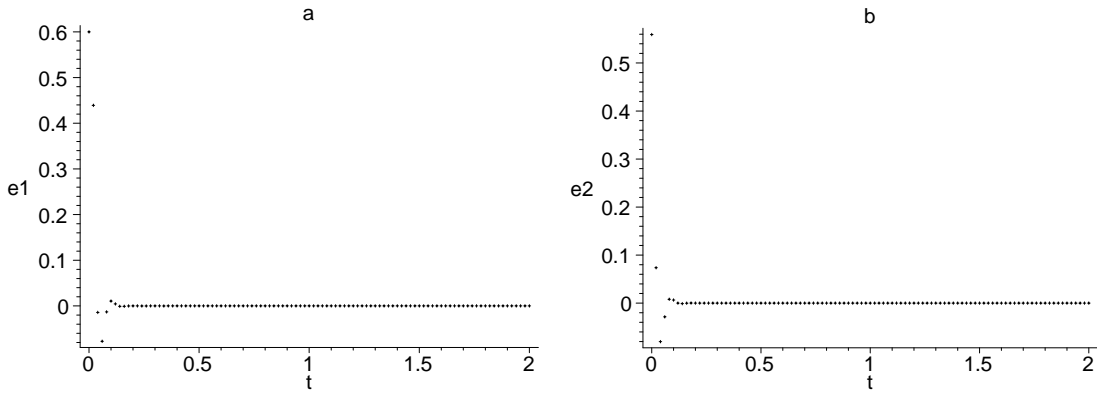


Fig. 2. Orbits of the error states. (a) The orbit of e_1 ; (b) the orbit of e_2 .

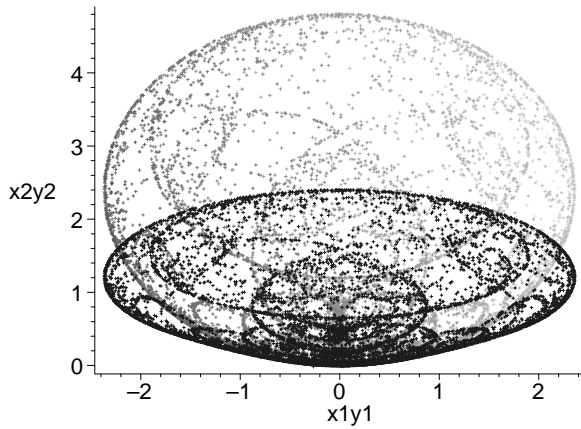


Fig. 3. Two attractors after being synchronized with $(f_1(x), f_2(x)) = (1, 1 + \tanh(x_2(k)))$: the dark one is the response system with the controllers, and the other one is the drive system.

(II): Let the error states be $E_1(k) = x_1(k) - 2y_1(k)$, $E_2(k) = x_2(k) - 2y_2(k)$, that is $f_1(x) = 2, f_2(x) = 2$. Similarly, from (3.1) and (3.2), we have the discrete-time error dynamical system

$$\begin{aligned} E_1(k+1) &= (1 + \alpha\beta)x_1(k) - \beta x_1(k)x_2(k) \\ &\quad - 2ay_1(k) - 2y_2(k) - 2u_1(x, y), \\ E_2(k+1) &= -2b + \beta x_1^2(k) + (1 - \beta)x_2(k) \\ &\quad - 2y_1^2(k) - 2u_2(x, y). \end{aligned} \quad (3.10)$$

Repeating the process in **(I)**, we get the attractors

$$\begin{aligned} u_1(x, y) &= \frac{1}{2}(1 + \alpha\beta - c_{11})x_1(k) - \frac{1}{2}\beta x_1(k)x_2(k) \\ &\quad - \frac{1}{2}x_2(k) + (c_{11} - a)y_1(k), \end{aligned}$$

$$\begin{aligned} u_2(x, y) &= -b - \frac{1}{2}c_{21}x_1(k) + \frac{1}{2}\beta x_1^2(k) \\ &\quad + \frac{1}{2}(1 - \beta - c_{22})x_2(k) - y_1^2(k) \\ &\quad + c_{21}y_1(k) + c_{22}y_2(k). \end{aligned} \quad (3.11)$$

Taking the same values of $[c_{11}, c_{21}, c_{22}, d_1]$ and the same initial values, we also use numerical simulations to verify the effectiveness of the above-mentioned controllers. The graphs of FPS error states and the global picture of the drive and response systems are displayed in Figs. 4a, 4b and 5.

4. FPS of the 3D Rössler Hyperchaotic System and the Hénon-Like Map

Consider the 3D hyperchaotic Rössler discrete-time system

$$\begin{aligned} x_1(k+1) &= 3.8x_1(k)(1 - x_1(k)) \\ &\quad - 0.05(x_3(k) + 0.35)(1 - 2x_2(k)), \\ x_2(k+1) &= 3.78x_2(k)(1 - x_2(k)) + 0.2x_3(k), \\ x_3(k+1) &= 0.1(1 - 1.9x_1(k)) \\ &\quad \cdot [(x_3(k) + 0.35)(1 - 2x_2(k)) - 1], \end{aligned} \quad (4.1)$$

and the 3D Hénon-like map

$$\begin{aligned} y_1(k+1) &= 1 + y_3(k) - \alpha y_2^2(k) + u_1(x, y), \\ y_2(k+1) &= 1 + \beta y_2(k) - \alpha y_1^2(k) + u_2(x, y), \\ y_3(k+1) &= \beta y_1(k) + u_3(x, y), \end{aligned} \quad (4.2)$$

as the drive system and response system, respectively.

Firstly we give out the figures (Fig. 6a and Fig. 6b) of the two systems with initial variables $[x_1(0) = 0.1, x_2(0) = 0.2, x_3(0) = -0.5]$ and $[y_1(0) = -0.5, y_2(0) =$

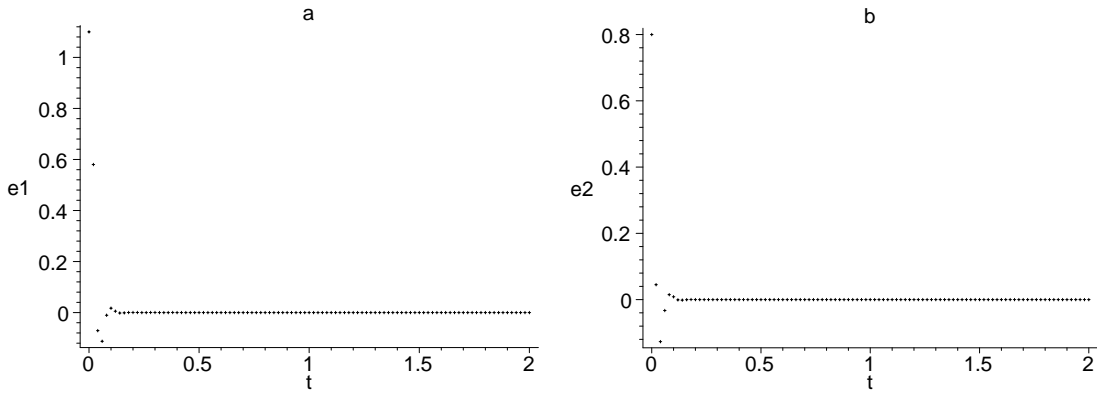


Fig. 4. Orbits of the error states. (a) The orbit of e_1 ; (b) the orbit of e_2 .

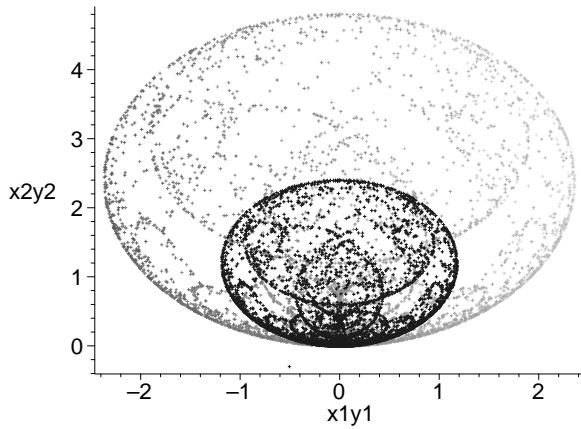


Fig. 5. Two attractors after being synchronized with $(f_1(x), f_2(x)) = (2, 2)$: the dark one is the response system with the controllers, and the other one is the drive system.

$0.2, y_3(0) = 0.1]$, respectively. Here $\alpha = 1.4$ and $\beta = 0.2$.

To realize the synchronization, let the error states be $E_1(k) = x_1(k) - (1 + x_1^2(k))y_1(k)/2$, $E_2(k) = x_2(k) + y_2(k)$, $E_3(k) = x_3(k) - 2y_3(k)$. Then from (4.1) and (4.2), we obtain the discrete-time error dynamical system 4.3

$$\begin{aligned}
 E_1(k+1) &= 3.8x_1(k)(1-x_1(k)) - 0.05(x_3(k)+0.35) \\
 &\cdot (1-2x_2(k)) - 0.05(x_3(k)+0.35)(1-2x_2(k)) \\
 &- (1+y_3(k) - \alpha y_2(k)^2 + u_1(x,y)) [1 + (3.8x_1(k) \\
 &\cdot (1-x_1(k)) - 0.05(x_3(k)+0.35)(1-2x_2(k)))^2] / 2, \\
 E_2(k+1) &= 3.78x_2(k)(1-x_2(k)) + 0.2x_3(k) + 1 \\
 &- \beta y_2(k) - \alpha y_1(k)^2 + u_2(x,y), \\
 E_3(k+1) &= 0.1(1-1.9x_1(k)) [(x_3(k)+0.35) \\
 &\cdot (1-2x_2(k)) - 1] - 2\beta y_1(k) - 2u_3(x,y). \quad (4.3)
 \end{aligned}$$

Based on the backstepping design method and Lyapunov stability theory, we can get the controllers step by step like in Section 3. Here we omit the concrete process. Finally, with the aid of symbolic computation, from

$$E_1(k) = x_1(k) - \frac{(1+x_1^2(k))}{2}y_1(k), \quad (4.4)$$

$$E_2(k) = E_1(k+1) - c_{11}E_1(k), \quad (4.5)$$

$$E_3(k) = E_2(k+1) - c_{21}E_1(k) - c_{22}E_2(k), \quad (4.6)$$

$$E_3(k+1) - c_{31}E_1(k) - c_{32}E_2(k) - c_{33}E_3(k) = 0, \quad (4.7)$$

we get the controllers $u_1(x,y), u_2(x,y)$ and $u_3(x,y)$:

$$\begin{aligned}
 u_1(x,y) &= [280x_3(k)\alpha y_2(k)^2 - 196x_2(k)\alpha y_2(k)^2 \\
 &- 1600x_3(k)^2x_2(k)^2y_3(k) + 196x_2(k)^2\alpha y_2(k)^2 \\
 &+ 2331680x_1(k)^2\alpha y_2(k)^2 - 121600x_1(k)x_3(k)x_2(k) \\
 &- 4620800x_1(k)^3\alpha y_2(k)^2 \\
 &+ 121600x_1(k)x_3(k)x_2(k)\alpha y_2(k)^2 - 320000c_{11}x_1(k) \\
 &- 121600x_1(k)^2x_3(k)x_2(k)\alpha y_2(k)^2 + 196x_2(k)y_3(k) \\
 &+ 160049\alpha y_2(k)^2 + 1237280x_1(k) - 16280x_3(k) \\
 &- 308604x_2(k) - 160049y_3(k) - 320000y_2(k) \\
 &- 3547680x_1(k)^2 - 1120x_3(k)x_2(k)\alpha y_2(k)^2 \\
 &- 1600x_3(k)^2x_2(k)\alpha y_2(k)^2 + 1600x_3(k)^2x_2(k)^2\alpha y_2(k)^2 \\
 &+ 1120x_3(k)x_2(k)^2\alpha y_2(k)^2 + 42560x_1(k)x_2(k)\alpha y_2(k)^2 \\
 &- 42560x_1(k)^2x_2(k)\alpha y_2(k)^2 - 60800x_1(k)x_3(k)\alpha y_2(k)^2 \\
 &+ 60800x_1(k)^2x_3(k)\alpha y_2(k)^2 \\
 &+ 121600x_1(k)^2x_3(k)x_2(k)y_3(k) \\
 &- 121600x_1(k)x_3(k)x_2(k)y_3(k) + 400\alpha x_3(k)^2y_2(k)^2 \\
 &+ 1600x_3(k)^2x_2(k)y_3(k) - 1120x_3(k)x_2(k)^2y_3(k) \\
 &+ 1120x_3(k)x_2(k)y_3(k) - 21280x_1(k)\alpha y_2(k)^2]
 \end{aligned}$$

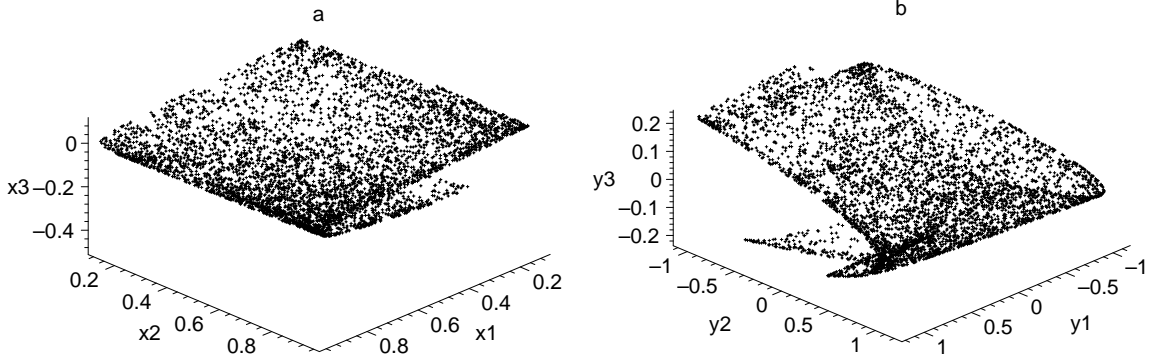


Fig. 6. (a) Attractor of the Rössler hyperchaotic system; (b) attractor of the Hénon-like map.

$$\begin{aligned}
& +121600x_1(k)^2x_3(k)x_2(k) + 160000c_{11}y_1(k)x_1(k)^2 \\
& +2310400\alpha x_1(k)^4y_2(k)^2 + 60800x_1(k)x_3(k)y_3(k) \\
& -42560x_1(k)x_2(k)y_3(k) + 42560x_1(k)^2x_2(k)y_3(k) \\
& -60800x_1(k)^2x_3(k)y_3(k) - 196x_2(k)^2 - 400x_3(k)^2 \\
& +4620800x_1(k)^3 - 2310400x_1(k)^4 + 160000c_{11}y_1(k) \\
& -196x_2(k)^2y_3(k) - 280x_3(k)y_3(k) - 400x_3(k)^2y_3(k) \\
& +33120x_3(k)x_2(k) + 1600x_3(k)^2x_2(k) \\
& -1600x_3(k)^2x_2(k)^2 - 1120x_3(k)x_2(k)^2 \\
& -2331680x_1(k)^2y_3(k) + 21280x_1(k)y_3(k) \\
& +4620800x_1(k)^3y_3(k) - 2310400x_1(k)^4y_3(k) \\
& -42560x_1(k)x_2(k) + 42560x_1(k)^2x_2(k) \\
& +60800x_1(k)x_3(k) - 60800x_1(k)^2x_3(k) - 165649 \\
& / [400x_3(k)^2 + 2310400x_1(k)^4 - 21280x_1(k) \\
& +280x_3(k) - 196x_2(k) - 4620800x_1(k)^3 + 196x_2(k)^2 \\
& +2331680x_1(k)^2 - 1120x_3(k)x_2(k) - 60800x_1(k)x_3(k) \\
& +42560x_1(k)x_2(k) + 60800x_1(k)^2x_3(k) \\
& -42560x_1(k)^2x_2(k) - 1600x_3(k)^2x_2(k) \\
& +1600x_3(k)^2x_2(k)^2 + 1120x_3(k)x_2(k)^2 + 160049 \\
& -121600x_1(k)^2x_3(k)x_2(k) + 121600x_1(k)x_3(k)x_2(k)],
\end{aligned}$$

$$\begin{aligned}
u_2(x, y) &= -1 + c_{21}x_1(k) + (-3.78 + c_{22})x_2(k) \\
& + 3.78x_2(k)^2 + 0.8x_3(k) - 0.5c_{21}(1 + x_1(k)^2)y_1(k) \\
& + \alpha y_1(k)^2 + (c_{22} - \beta)y_2(k) - 2y_3(k),
\end{aligned}$$

$$\begin{aligned}
u_3(x, y) &= (0.06175 - 0.5c_{31})x_1(k) \\
& + (0.5c_{32} - 0.035)x_2(k) + 0.5(1 - c_{33})x_3(k) \\
& - 0.1x_2(k)x_3(k) - 0.095x_1(k)x_3(k) \\
& + 0.19x_1(k)x_2(k)x_3(k) + 0.0665x_1(k)x_2(k) \\
& - (\beta - 0.25c_{31})y_1(k) - 0.5c_{32}y_2(k) + c_{33}y_3(k) \\
& - 0.0325 + 0.25c_{31}y_1(k)x_1(k)^2.
\end{aligned}$$

Let the Lyapunov function be $L(k) = |E_1(k)| + d_1|E_2(k)| + d_2|E_3(k)|$, $d_2 > d_1 > 1$. Then from (4.4), (4.5), (4.6) and (4.7), we obtain the derivative of the Lyapunov function $L(k)$:

$$\begin{aligned}
\Delta L(k) &= L(k+1) - L(k) \\
&\leq (d_2|c_{31}| + d_1|c_{21}| + |c_{11}| - 1)|E_1(k)| \\
&\quad + (d_2|c_{32}| + d_1(|c_{22}| - 1) + 1)|E_2(k)| \\
&\quad + (d_2|c_{33}| + d_1 - d_2)|E_3(k)|.
\end{aligned}$$

If we set the constants c_{11} , c_{21} , c_{22} , c_{31} , c_{32} , c_{33} to satisfy

$$\begin{aligned}
d_1|c_{21}| + d_2|c_{31}| + |c_{11}| &< 1, \\
d_1|c_{22}| + d_2|c_{32}| &< d_1 - 1, \\
|c_{33}| &< \frac{d_2 - d_1}{d_2},
\end{aligned}$$

then $\Delta L(k)$ is negative definite which denotes that the resulting close-loop discrete-time system

$$\begin{pmatrix} E_1(k+1) \\ E_2(k+1) \\ E_3(k+1) \end{pmatrix} = \begin{pmatrix} c_{11} & 1 & 0 \\ c_{21} & c_{22} & 1 \\ c_{31} & c_{32} & c_{33} \end{pmatrix} \begin{pmatrix} E_1(k) \\ E_2(k) \\ E_3(k) \end{pmatrix}$$

is globally asymptotically stable and $\lim_{k \rightarrow +\infty} E_i(k) = 0$, that is to say, the hyperchaotic Rössler discrete-time system (4.1) and the Hénon-like map (4.2) are function projective synchronized.

In the following we use numerical simulations to verify the effectiveness of the obtained controllers $u(x, y)$. Here take $c_{11} = 0.3$, $c_{21} = 0.02$, $c_{22} = 0.4$, $c_{31} = 0.05$, $c_{32} = 0.1$, $c_{33} = -0.2$, $d_1 = 4$, $d_2 = 6$, and the initial values $[x_1(0) = 0.1, x_2(0) = 0.2, x_3(0) = -0.5]$ and $[y_1(0) = -0.5, y_2(0) = 0.2, y_3(0) = 0.1]$, respectively. The graphs of the error states are shown

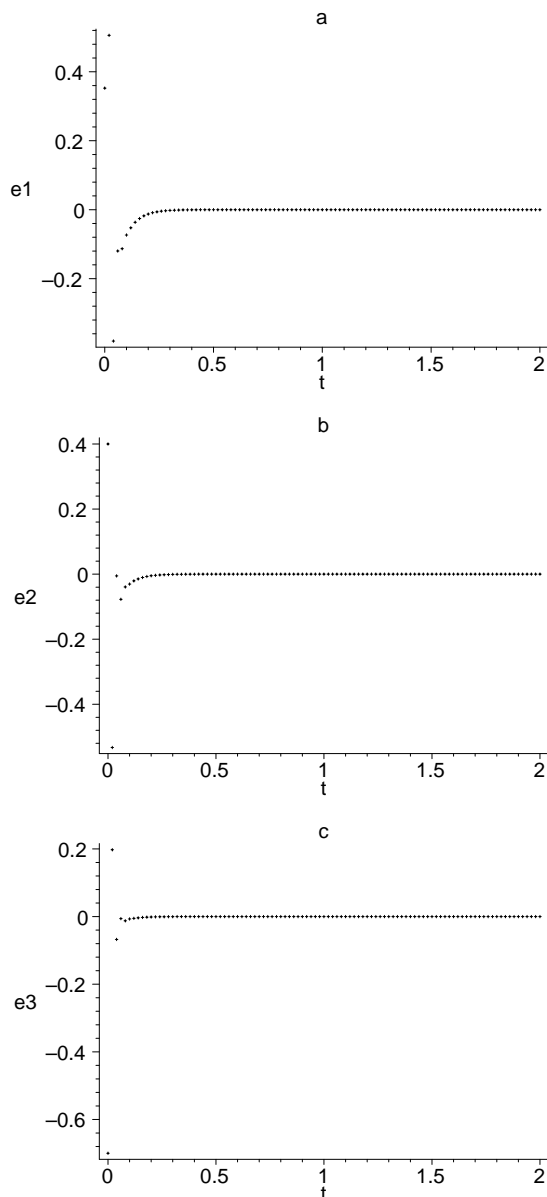


Fig. 7. Orbits of the error states. (a) The orbit of e_1 ; (b) the orbit of e_2 ; (c) the orbit of e_3 .

in Figs. 7a–c, and the attractors of the two systems with controllers are displayed in Figure 8.

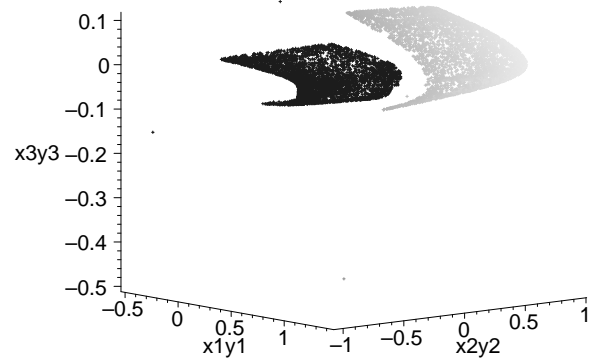


Fig. 8. Two attractors after being synchronized with $(f_1(x), f_2(x), f_3(x)) = ((1+x_1^2)/2, -1, 2)$: the dark one is the response system with the controllers, and the other one is the drive system.

5. Summary and Conclusions

We have defined the function projective synchronization in discrete-time dynamical systems. Then based on backstepping design with controllers, a systematic and automatic scheme was developed to investigate the FPS between the discrete-time drive systems and response systems with strict feedback forms. Moreover the proposed scheme was used to illustrate the function projective synchronization between the 2D Lorenz discrete-time system and the Fold system, as well as the 3D hyperchaotic Rössler discrete-time system and the Hénon-like map. Numerical simulations were used to verify the effectiveness of the proposed scheme.

Acknowledgements

The authors would like to express their thanks to Yunqing Yang for providing references and help. The work is supported by the National Natural Science Foundation of China (Grant No. 10735030), Shanghai Leading Academic Discipline Project (No. B412), Zhejiang Provincial Natural Science Foundations of China (Grant No. Y604056), Doctoral Foundation of Ningbo City (No. 2005A61030) and Program for Changjiang Scholars and Innovative Research Team in University (IRT0734).

- [1] H. Fujisaka and T. Yamada, *Prog. Theor. Phys.* **69**, 32 (1983).
 [2] L. M. Pecora and T. L. Carroll, *Phys. Rev. Lett.* **64**, 821 (1990); T. L. Carroll and L. M. Pecora, *IEEE Trans. Circuits Syst., I: Fundam. Theory Appl.* **38**, 453 (1991).

- [3] K. Pyragas, *Phys. Lett. A* **170**, 421 (1992); **181**, 203 (1993).
 [4] E. Ott, C. Grebogi, and J. A. Yorke, *Phys. Rev. Lett.* **64**, 1196 (1990).

- [5] S. Boccaletti, J. Kurth, G. Osipov, D. L. Valladares, and C. S. Zhou, *Phys. Rep.* **366**, 1 (2002).
- [6] L. Kocarev and U. Parlitz, *Phys. Rev. Lett.* **76**, 1816 (1996).
- [7] R. Brown and L. Kocarev, *Chaos* **10**, 344 (2000).
- [8] S. Boccaletti, L. M. Pecora, and A. Pelaez, *Phys. Rev. E* **63**, 066219 (2001).
- [9] T. Kapitaniak, *Phys. Rev. E* **50**, 1642 (1994); T. Kapitaniak, L. O. Chua, and G. Q. Zhong, *Int. J. Bifur. Chaos* **6**, 211 (1996).
- [10] G. Chen and X. Dong, *From Chaos to Order*, World Scientific, Singapore 1998.
- [11] Z. Y. Yan, *Chaos* **15**, 023902 (2005); *Chaos, Solitons and Fractals* **334**, 406 (2005).
- [12] R. Mainieri and J. Rehacek, *Phys. Rev. Lett.* **82**, 3042 (1999).
- [13] J. Yan and C. Li, *Chaos, Solitons and Fractals* **26**, 1119 (2005).
- [14] G. Wen and D. Xu, *Chaos, Solitons and Fractals* **26**, 71 (2005).
- [15] G. H. Li, *Chaos, Solitons and Fractals* **32**, 1454 (2007).
- [16] Y. Chen and X. Li, *Z. Naturforsch.* **62a**, 176 (2007).
- [17] X. Y. Wang, *Chaos in Complex Nonlinear Systems*, Publishing House of Electronics Industry, Beijing 2003; T. Yamakawa, T. Miki, and E. Uchino, *Proceedings of the 2nd International Conference on Fuzzy Logic and Neural Networks*, Iizuka, Japan, July 1992, pp. 563 – 566.
- [18] M. Hénon, *Commun. Math. Phys.* **50**, 69 (1976); K. Stefanski, *Chaos, Solitons and Fractals* **9**, 93 (1998); G. Baier and M. Klain, *Phys. Lett. A* **151**, 281 (1990); N. F. Rulkov, *Phys. Rev. Lett.* **86**, 183 (2001).
- [19] M. Itoh, T. Yang, and L. O. Chua, *Int. J. Bifurcation Chaos Appl. Sci. Eng.* **11**, 551 (2001); K. Konishi and H. Kokame, *Phys. Lett. A* **248**, 359 (1998); M. Itoh and L. O. Chua, *Int. J. Bifurcation Chaos Appl. Sci. Eng.* **13**, 1055 (2003); J. Douglass, L. Wilkens, E. Pantazelou, and F. Moss, *Nature (London)* **365**, 337 (1993).
- [20] G. M. Zaslavsky, M. Edelman, and B. A. Niyazov, *Chaos* **7**, 159 (1997); A. Becker and P. Eckelt, *Chaos* **3**, 487 (1993); M. Itoh and H. Murakami, *IEICE Trans. Fundamentals E* **77**, 2092 (1994).
- [21] Z. Y. Yan, *Chaos* **16**, 013119 (2006); *Phys. Lett. A* **342**, 309 (2005).
- [22] I. Kanellakopoulos, P. V. Kokotovic, and A. S. Morse, *IEEE Trans. Autom. Control* **36**, 1241 (1991).
- [23] M. Krstic, I. Kaneuakopoulos, and P. V. Kokotovic, *Nonlinear Adaptive Control Design*, Wiley, New York 1995.
- [24] C. Wang and S. S. Ge, *Chaos, Solitons and Fractals* **12**, 1199 (2001).
- [25] Q. Wang and Y. Chen, *Appl. Math. Comp.* **181**, 48 (2006).
- [26] C. Wang and S. S. Ge, *Int. J. Bifurcation Chaos Appl. Sci. Eng.* **11**, 1115 (2001).
- [27] S. H. Chen, D. Wang, L. Chen, Q. Zhang, and C. Wang, *Chaos* **14**, 539 (2004).
- [28] P. C. Yeh and P. V. Kokotovic, *Int. J. Control* **62**, 303 (1995).
- [29] J. Lu, R. Wei, X. Wang, and Z. Wang, *IEEE Trans. Circuits Syst., I: Fundam. Theory Appl.* **48**, 1359 (2001).
- [30] S. S. Ge, G. Y. Li, and T. H. Lee, *Automatica* **39**, 807 (2003).
- [31] L. Huang, M. Wang, and R. Feng, *Chaos, Solitons and Fractals* **23**, 617 (2005).